*Article*

# Theoretical Study of *closo*-Borate Anions $[B_nH_n]^{2-}$ (*n* = 5–12): Bonding, Atomic Charges, and Reactivity Analysis

**Ilya N. Klyukin [1],*, Yulia S. Vlasova [2] , Alexander S. Novikov [3] , Andrey P. Zhdanov [1] , Konstantin Y. Zhizhin [1] and Nikolay T. Kuznetsov [1]**

[1] Kurnakov Institute of General and Inorganic Chemistry, Russian Academy of Sciences, Leninskii pr. 31, 117907 Moscow, Russia; zhdanov@igic.ras.ru (A.P.Z.); zhizhin@igic.ras.ru (K.Y.Z.); ntkuz@igic.ras.ru (N.T.K.)

[2] Faculty of Chemistry, Lomonosov Moscow State University, Leninskiye Gory GSP-1, 1-3, 119991 Moscow, Russia; iuliia.vlasova@chemistry.msu.ru

[3] Institute of Chemistry, Saint Petersburg State University, Universitetskaya Nab. 7-9, 199034 Saint Petersburg, Russia; a.s.novikov@spbu.ru

* Correspondence: klukinil@gmail.com or klukinil@igic.ras.ru

**Abstract:** This study has focused on the structure, bonding, and reactivity analysis of *closo*-borate anions $[B_nH_n]^{2-}$ (*n* = 5–12). Several descriptors of B–H interactions have been calculated. It has been found that the values of electron density and total energy at bond critical point are the most useful descriptors for investigation of B–H interactions. Using results from the descriptor analysis, one may conclude that orbital interactions in $[B_nH_n]^{2-}$ increase with increasing the boron cluster size. Several approaches to estimate atomic charges have been applied. Boron atoms in apical positions have more negative values of atomic charges as compared with atoms from equatorial positions. The mean values of boron and hydrogen atomic charges tend to be more positive with the increasing of boron cluster size. Global and local reactivity descriptors using conceptual density functional theory (DFT) theory have been calculated. Based on this theory, the *closo*-borate anions $[B_nH_n]^{2-}$ (*n* = 5–9) can be considered strong and moderate electrophiles, while the *closo*-borate anions $[B_nH_n]^{2-}$ (*n* = 10–12) can be considered marginal electrophiles. Fukui functions for electrophilic attack have been calculated. Fukui functions correlate well with atomic charges of the *closo*-borate anions. Boron atoms in apical positions have the most positive values of Fukui functions.

**Keywords:** DFT; closo-borate anions; reactivity descriptors; QTAIM analysis; Fukui functions

## 1. Introduction

The *closo*-borate anions of general formula $[B_nH_n]^{2-}$ (*n* = 5–12) have been extensively studied theoretically and experimentally [1–4]. These cluster species have highly symmetrical structure and unusual chemical bonding, which cannot be described by classical Lewis structure [5–7]. *closo*-borate anions and their derivatives have a lot of useful features such as high stability, low toxicity, and magnetic properties [8–11]. The main application of *closo*-borate anions is boron neutron capture therapy of cancer [12–14]. In addition, these anions have a lot of potential applications in photochemistry, medicine, and electrochemistry [15–17].

*closo*-borate anions of general formula $[B_nH_n]^{2-}$ (*n* = 5–12) are convenient building blocks for formatting inorganic and bioinorganic systems with desired properties [18–21]. The possibility to substitute terminal hydrogen atom with *exo*-polyhedral groups allows one to obtain various derivatives of *closo*-borate anions. There are a lot of approaches to functionalize this type of anions [22–25]. Among these approaches, the most convenient and studied is electrophile-induced nucleophilic substitution (EINS) [26,27].

Currently, many useful methods focused on structure and reactivity analysis have been described. The quantum theory of atoms in molecules (QTAIM) analysis gives clear information about covalent and non-covalent interactions [28–30]. Previously, several

*closo*-borate anions have been calculated by QTAIM analysis [31,32]. The main focus in these studies has been directed to B-B interactions and the investigation of the *exo*-polyhedral bonds of the general type B-X, where X = C, O, N [33–35]. Conceptual density functional theory (DFT) allows one to obtain information about reactivity using only values of highest occupied molecular orbital (HOMO)-lowest unoccupied molecular orbital (LUMO) energies [36–39]. Fukui functions allow one to obtain information about molecular reactivity site [40–42]. Some main conceptual DFT descriptors of *closo*-borate anions $[B_nH_n]^{2-}$ ($n$ = 5–12) have been calculated [43], but the most convenient index for estimation reactivity—electrophilicity index—remains undiscussed.

In present work, we have focused on the comprehensive investigation of *closo*-borate anions $[B_nH_n]^{2-}$ ($n$ = 5–12). The study of B–H bonds allows one to obtain information about their stability and possibility to break in substitution reactions. Using several bonding descriptors, we have found main trends in the B-H interactions. Calculation of atomic charges allows one to obtain information about electronic density distribution in molecules. In the present work, several approaches to estimate atomic charges have been used.

For finding main trends in reactivity of the *closo*-borate anions, conceptual density functional theory (DFT) has been used. As shown previously, the most interesting reaction type for *closo*-borate-anions is the EINS process. In these reactions, complexes with Lewis acids are formed on the first stage. As electrophile inductor $H^+$, carbocations and $AlCl_3$ can be used [44,45]. For finding most suitable site for electrophilic attack, Fukui functions have been used.

## 2. Materials and Methods

*Computational Details*

The full geometry optimization procedure for all model structures has been performed at the ωB97X-D3/6-31++G(d,p) level of theory [46,47]. Note that ωB97X-D3 functional provides accurate results for QTAIM analysis, charge density distribution, and conceptual DFT descriptors in a satisfactory level [48–50], and we already successfully applied this DFT functional in similar theoretical studies of different boron clusters chemical systems [33–35]. Tight SCF (self-consistent field) convergence has been employed during the calculations. All computations have been performed with the help of the ORCA 4.2.1 program package [51]. All the *closo*-borate anions $[B_nH_n]^{2-}$ ($n$ = 5–12) have closed electron shells, thus the spin restricted approximation has been applied for all structures. Symmetry operations have not been applied during the geometry optimization procedures for all structures. All stationary points on the potential energy surfaces have been characterized as minima by eigenvalue analysis of the diagonalized Hessians (no imaginary frequencies). The natural population analysis and natural bond orbital (NBO) calculations has been performed by using NBO7 program package [52]. The topological analysis of the electron density according to quantum theory of atoms in molecules (QTAIM) formalism developed by Bader [53] has been carried out with the Multiwfn program (version 3.7) [54]. The main reactivity indices (electronic chemical potential $\mu$, chemical hardness $\eta$, and softness $S$, global electrophilicity $\omega$) have been calculated using the Equations (1)–(4) [55]:

$$\mu = \frac{E_{HOMO} + E_{LUMO}}{2} \tag{1}$$

$$\eta = E_{LUMO} - E_{HOMO} \tag{2}$$

$$S = \frac{1}{\eta} \tag{3}$$

$$\omega = \frac{\mu^2}{2\eta} \tag{4}$$

The condensed Fukui functions ($f_k{}^+$) have been calculated with the help of natural population analysis (NPA), Hirshfeld, and AIM charges using the following equation:

$$f_k^+ = q_k(anion) - q_k(neutral)$$

where $q_k$ (anion) and $q_k$ (neutral) are the charges at atom $k$ on the anion and neutral species, respectively.

## 3. Results and Discussion

### 3.1. B–H Bond

We have investigated the B–H bond phenomena in *closo*-borate anions of general formula $[B_nH_n]^{2-}$ ($n$ = 5–12). Optimized structures of the *closo*-borate anions are shown in Figure 1. Several common descriptors have been used. First, the B-H bond lengths were inspected. We found that the lengths of B–H bonds lie in a tight interval between 1.21–1.22 Å, and this observation correlates well with previous theoretical and experimental studies [31,56,57]. The Wiberg bond index is another useful and convenient descriptor for investigation bond phenomena. The Wiberg bond indices of B–H bonds in *closo*-borate anions fall in the range 0.93–0.96. The B–H bonding interactions in the *closo*-borate anions $[B_nH_n]^{2-}$ ($n$ = 5–12) were theoretically investigated using the QTAIM approach, and main local and integral topological properties of the electron density involved in these interactions were computed. For main topological parameters of electron density for B–H interactions, see Supporting Information, Table S1.
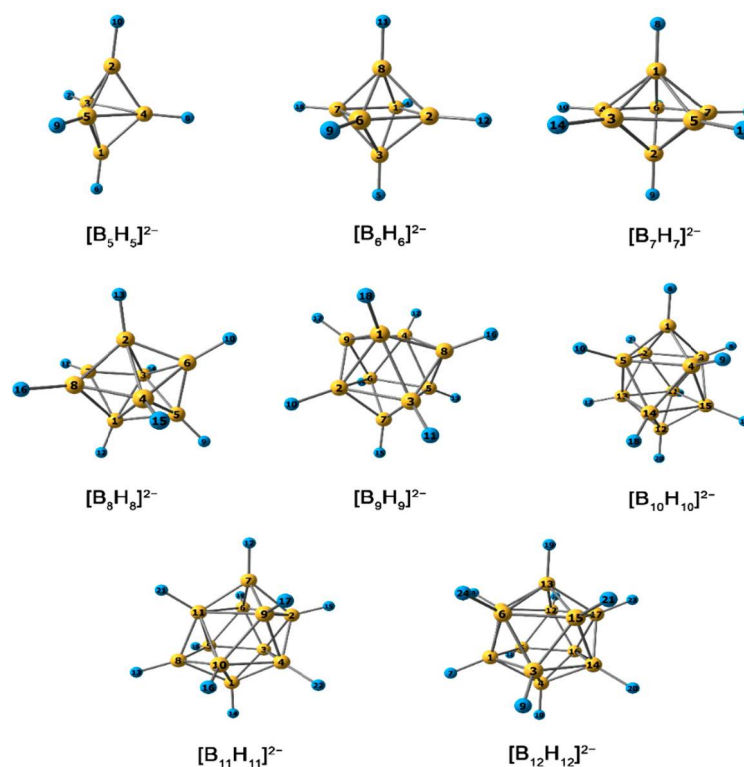


**Figure 1.** Optimized structures of the *closo*-borate anions of general form $[B_nH_n]^{2-}$ ($n$ = 5–12).

As seen in Table S1, the value of p(r) at B–H bond critical points (bcp) increases with increasing the cluster size. Mean values of p(r) at B–H bond critical points (bcp) for each type of *closo*-borate anion are shown in Figure 2. Values $\nabla^2$p(r) for all types of *closo*-borate anions are negative. The most negative values have the $[B_{12}H_{12}]^{2-}$ anion. All B–H bcps are characterized by negative values of total energy. B–H bcp between B(10) and H atom from $[B_{11}H_{11}]^{2-}$ have the most negative value of total energy. We found a good correlation

between p(r) at bcp and value of total energy (Figure 3). The values of delocalization index for B–H interactions are not correlated with other descriptors and thus not useful for investigation of given types of bonds. The values of the main topological parameters for B–H interaction are typical for shared interactions.
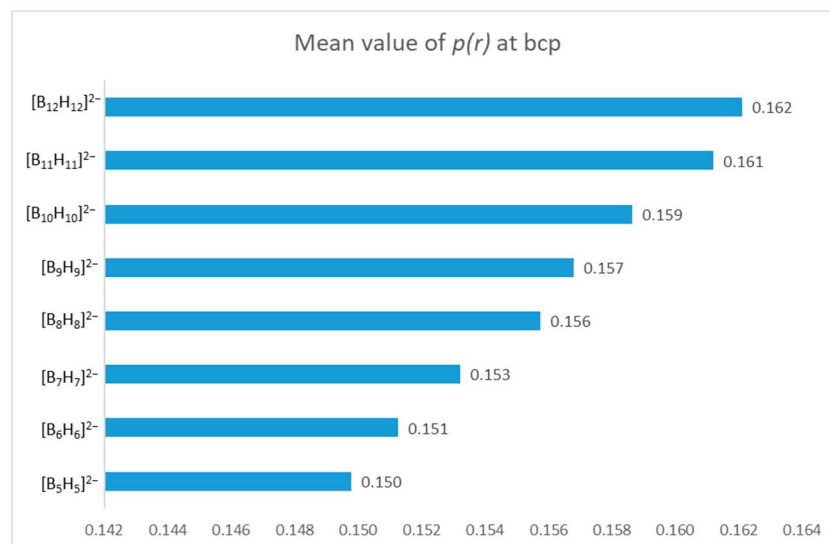
**Figure 2.** Values of electron density p(r) at bond critical points for the *closo*-borate anions of general formula $[B_nH_n]^{2-}$ ($n$ = 5–12).
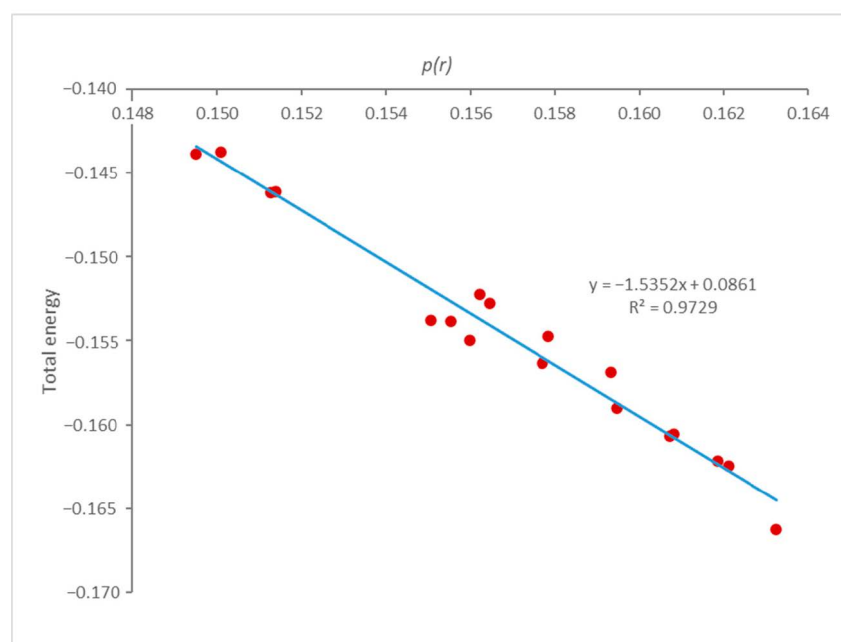
**Figure 3.** Correlation between values of total energy and electron density p(r) at B–H bond critical points.

Several bond descriptors of the B–H interactions in $[B_nH_n]^{2-}$ ($n$ = 5–12) have been elaborated. We found that using the values of the B–H bond length and Wiberg bond index does not allow one to obtain information about general trends of the B–H interaction phenomena, because these descriptors are not sensitive to the nature of *closo*-borate polyhedra and lie in tight intervals. Furthermore, the delocalization indices for B–H interactions have no correlation with other descriptors, so they are not convenient for investigation of the B–H bond phenomena. The values of electron density and total energy at bcp are the most

useful for investigation of B–H interactions. These two types of descriptors correlate well with the nature of the boron cluster. Summarizing all results from descriptor analysis, one may conclude that orbital interactions in $[B_nH_n]^{2-}$ increase with increasing boron cluster size.

### 3.2. Atomic Charges

We estimated atomic charges of $[B_nH_n]^{2-}$ ($n$ = 5–12) using AIM, NBO, and Hirshfeld approaches (Table S3). These methods give quite different results for values of atomic charges. In the case of the AIM method, there is a pronounced difference between boron and hydrogen atomic charges. Boron atoms have positive values of atomic charges, while hydrogen atoms have negative values. In the case of NBO atomic charges, we found the opposite situation: boron atoms have more negative charges than hydrogen atoms. In the case of Hirshfeld method, boron and hydrogen atoms have similar values of atomic charges. The mean values of Hirshfeld atomic charges for boron atoms are shown in Figure 4 (for hydrogen atoms, see Figure S1). However, despite these peculiar properties of each method, the main trends are the same. Initially, we found trends for each type of boron cluster. For symmetrical clusters ($[B_6H_6]^{2-}$ and $[B_{12}H_{12}]^{2-}$), all values of boron atomic charges are equal. In case of $[B_5H_5]^{2-}$ and $[B_{10}H_{10}]^{2-}$ anions, the most negative values of atomic charges are localized on apical boron atoms. In the case of $[B_7H_7]^{2-}$ anion, equatorial boron atoms have more negative value than apical boron atoms. For $[B_8H_8]^{2-}$ anion, boron atoms in positions B5–B8 have the most negative values. The boron atom in apical position and atoms B(8) and B(9) have the most negative value of atomic charges in $[B_9H_9]^{2-}$. For $[B_{11}H_{11}]^{2-}$, B(8) atom in apical position and atom B7 have most negative value of atomic charges. The values of atomic charges for hydrogen atoms are equal for all types of the clusters. We have calculated the mean values of atomic charges for each types of atoms for all *closo*-borate anions. Using mean values of atomic charges is simple approach to find general trends. We have found that with the increasing of boron cluster size, the mean values of boron and hydrogen atomic charges become more positive.
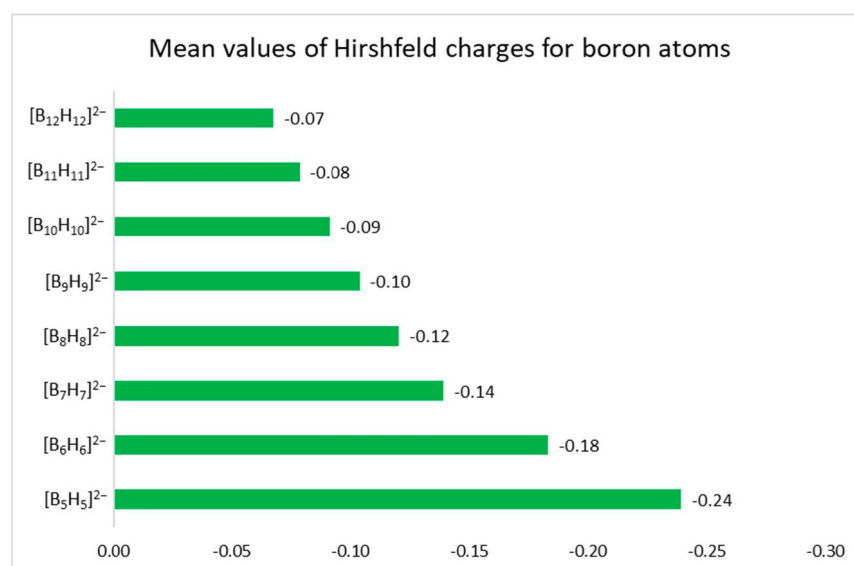


**Figure 4.** Mean values of Hirshfeld charges for boron atoms for the *closo*-borate anions of general form $[B_nH_n]^{2-}$ ($n$ = 5–12).

Different estimating methods give different results, but main trends are the same for all approaches. In general, boron atoms in apical positions have more negative values of atomic charges as compared atoms from equatorial positions. The mean values of boron and hydrogen atomic charges tend to be more positive with increasing boron cluster size.

Thus, the $[B_5H_5]^{2-}$ anion has the most negative values of mean B and H atomic charges, and the $[B_{12}H_{12}]^{2-}$ anion has the most positive values of mean B and H atomic charges.

### 3.3. Reactivity Analysis

The main reactivity indices obtained from Equation (1) for a series of *closo*-borate anions $[B_nH_n]^{2-}$ ($n$ = 5–12) are shown in Table S2.

The value of the HOMO-LUMO gap is increasing with increasing the boron cluster size. The $[B_{12}H_{12}]^{2-}$ anion has the most positive value of the HOMO-LUMO gap. The value of chemical potential $\mu$ has reverse trend, whereas the $[B_5H_5]^{2-}$ anion has the most positive value. The $[B_{12}H_{12}]^{2-}$ anion has the most positive value of chemical hardness $\eta$. Electrophilicity $\omega$ index value is decreasing with increasing the boron cluster size (Figure 5).
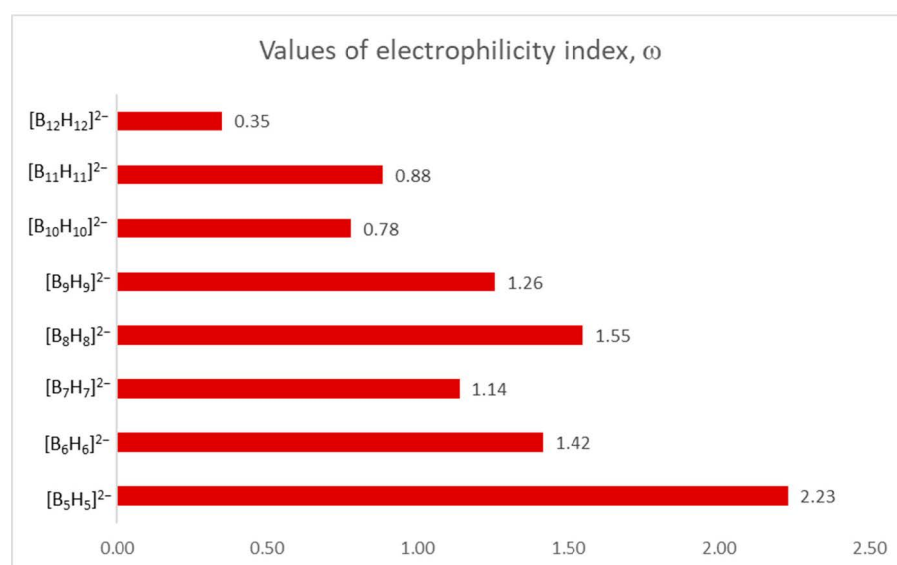


**Figure 5.** Values of electrophilicity index, $\omega$ for the *closo*-borate anions of general form $[B_nH_n]^{2-}$ ($n$ = 5–12).

Thus, based on the classification proposed by Domingo et al. [58,59] (electrophiles: $\omega > 1.50$ eV strong, $1.50 > \omega > 0.80$ eV moderate, $\omega < 0.80$ eV marginal), the *closo*-borate anions $[B_nH_n]^{2-}$ ($n$ = 5–9) can be considered strong and moderate electrophiles, and the *closo*-borate anions $[B_nH_n]^{2-}$ ($n$ = 10–12) can be considered marginal electrophiles.

### 3.4. Fukui Functions

We calculated Fukui functions for electrophilic attack using the AIM, NBO, and Hirshfeld approaches (Table S4). Cartesian coordinates of all optimized structures are given in the Table S5. Applying AIM charges leads to a lot of negative values of Fukui function, which are meaningless. For *closo*-borate anions, the more appropriate approaches to estimate Fukui functions are the Hirshfeld and NBO methods. These two methods have equal trends. For all types of anions, the boron atoms have the most positive values of Fukui functions. For $[B_5H_5]^{2-}$ and $[B_{10}H_{10}]^{2-}$ anions, boron atoms in apical positions have the most positive values of Fukui functions. For symmetrical cluster ($[B_6H_6]^{2-}$, $[B_{12}H_{12}]^{2-}$), all boron atoms are equal, but the values of Fukui functions are different. In the case of $[B_7H_7]^{2-}$, two equatorial boron atoms have the most positive values of Fukui functions. For $[B_8H_8]^{2-}$ anion, boron atoms B5–B8 have the most positive values of Fukui functions. The boron atom in apical position and atoms B8 and B9 have the most negative values of atomic charges in $[B_9H_9]^{2-}$. For $[B_{11}H_{11}]^{2-}$, atom in apical position B(8) and atom B(7) have the most positive values of Fukui functions. Thus, the values of Fukui function have similar trends with atomic charges. Atoms with the most negative values of atomic charges have the most values of Fukui functions.

Thus, Fukui function is a powerful descriptor to estimate the most probable sites of electrophilic attack for $[B_nH_n]^{2-}$ anions ($n = 5$–$12$). The best way to estimate this descriptor is using the NBO and Hirshfeld approaches. Fukui functions correlate well with atomic charges of the *closo*-borate anions. In general, boron atoms in apical positions have the most positive values of Fukui functions.

## 4. Conclusions

A comprehensive investigation of the *closo*-borate anions of general formula $[B_nH_n]^{2-}$ ($n = 5$–$12$) has been carried out. Several descriptors of B–H interactions have been calculated. It has been found that the values of electron density and total energy at bond critical point are the most useful descriptors for investigation of B–H interactions. These two types of descriptors correlate well with the nature of the boron cluster. Summarizing all results from the descriptor analysis, one may conclude that orbital interactions in $[B_nH_n]^{2-}$ increase with increasing the boron cluster size. Several approaches to estimate atomic charges have been applied. In general, boron atoms in apical positions have more negative values of atomic charges as compared with atoms from equatorial positions. The mean values of boron and hydrogen atomic charges tend to be more positive with the increasing of boron cluster size. Global and local reactivity descriptors using conceptual DFT theory have been calculated. Based on this theory, the *closo*-borate anions $[B_nH_n]^{2-}$ ($n = 5$–$9$) can be considered strong and moderate electrophiles, while the *closo*-borate anions $[B_nH_n]^{2-}$ ($n = 10$–$12$) can be considered marginal electrophiles. Fukui functions for electrophilic attack have been calculated. The best way to estimate this descriptor is using the NBO and Hirshfeld approaches. Fukui functions correlate well with atomic charges of the *closo*-borate anions. In general, boron atoms in apical positions have the most positive values of Fukui functions.

## Abbreviations

| | |
|---|---|
| AIM | atoms in molecules |
| Bcp | bond critical points |
| DFT | density functional theory |
| EINS | electrophile-induced nucleophilic substitution |
| HOMO | highest occupied molecular orbital |
| LUMO | lowest unoccupied molecular orbital |
| NBO | natural bond orbitals |
| NPA | natural population analysis |
| QTAIM | quantum theory of atoms in molecules |

## References

1.  Golub, I.E.; Filippov, O.A.; Kulikova, V.A.; Belkova, N.V.; Epstein, L.M.; Shubina, E.S. Thermodynamic Hydricity of Small Borane Clusters and Polyhedral closo-Boranes. *Molecules* **2020**, *25*, 2920. [CrossRef] [PubMed]
2.  Muetterties, E.L. Chemistry of Boranes. XVIII. *Inorg. Chem.* **1964**, *231*, 1450–1456.
3.  Hawthorne, M.F.; Mavunkal, I.J.; Knobler, C.B. Electrophilic Reactions of Protonated closo -$B_{10}H_{10}{}^{2-}$ with Arenes, Alkane C-H Bonds, and Triflate Ion Forming Aryl, Alkyl, and Triflate nido -6-X-$B_{10}H_{13}$ Derivatives. *J. Am. Chem. Soc.* **1992**, *9*, 4427–4429. [CrossRef]
4.  Bondarev, O.; Sevryugina, Y.V.; Jalisatgi, S.S.; Hawthorne, M.F. Acid-Induced Opening of [closo-$B_{10}H_{10}]^{2-}$ as a New Route to 6-Substituted nido-$B_{10}H_{13}$ Decaboranes and Related Carboranes. *Inorg. Chem.* **2012**, *51*, 9935–9942. [CrossRef]
5.  Hoffmann, R.; Lipscomb, W.N. Theory of polyhedral molecules. I. Physical factorizations of the secular equation. *J. Chem. Phys.* **1962**, *36*, 2179–2189. [CrossRef]
6.  Lipscomb, W.N. Framework Rearrangement in Boranes and Carboranes. *Science* **1966**, *153*, 373–378. [CrossRef] [PubMed]
7.  Lipscomb, W.N. The Boranes and Their Relatives. *Science* **1977**, *196*, 1047–1055. [CrossRef] [PubMed]
8.  Mu, X.; Axtell, J.C.; Bernier, N.A.; Kirlikovali, K.O.; Jung, D.; Umanzor, A.; Qian, K.; Chen, X.; Bay, K.L.; Kirollos, M.; et al. Sterically Unprotected Nucleophilic Boron Cluster Reagents. *Chem* **2019**, *5*, 2461–2469. [CrossRef]
9.  Keener, M.; Hunt, C.; Carroll, T.G.; Kampel, V.; Dobrovetsky, R.; Hayton, T.W.; Ménard, G. Redox-switchable carboranes for uranium capture and release. *Nature* **2020**, *577*, 652–655. [CrossRef]
10.  Černý, R.; Brighi, M.; Murgia, F. The Crystal Chemistry of Inorganic Hydroborates. *Chemistry* **2020**, *2*, 805–826. [CrossRef]
11.  Didelot, E.; Łodziana, Z.; Murgia, F.; Černý, R. Ethanol- and Methanol-Coordinated and Solvent-Free Dodecahydro closo-Dodecaborates of 3d Transition Metals and of Magnesium. *Crystals* **2019**, *9*, 372. [CrossRef]
12.  Hu, K.; Yang, Z.; Zhang, L.; Xie, L.; Wang, L.; Xu, H.; Josephson, L.; Liang, S.H.; Zhang, M.R. Boron agents for neutron capture therapy. *Coord. Chem. Rev.* **2020**, *405*, 213139. [CrossRef]
13.  Nakagawa, F.; Kawashima, H.; Morita, T.; Nakamura, H. Water-Soluble closo-Docecaborate-Containing Pteroyl Derivatives Targeting Folate Receptor-Positive Tumors for Boron Neutron Capture Therapy. *Cells* **2020**, *9*, 1615. [CrossRef]
14.  Goswami, L.N.; Ma, L.; Chakravarty, S.; Cai, Q.; Jalisatgi, S.S.; Hawthorne, M.F. Discrete Nanomolecular Polyhedral Borane Scaffold Supporting Multiple Gadolinium(III) Complexes as a High Performance MRI Contrast Agent. *Inorg. Chem.* **2013**, *52*, 1694–1700. [CrossRef]
15.  Ali, F.; Hosmane, N.S.; Zhu, Y. Boron Chemistry for Medical Applications. *Molecules* **2020**, *25*, 828. [CrossRef]
16.  Axtell, J.C.; Messina, M.S.; Liu, J.Y.; Galaktionova, D.; Schwan, J.; Porter, T.M.; Savage, M.D.; Wixtrom, A.I.; Rheingold, A.L.; Kubiak, C.P.; et al. Photooxidative generation of dodecaborate-based weakly coordinating anions. *Inorg. Chem.* **2019**, *58*, 10516–10526. [CrossRef] [PubMed]
17.  Duchêne, L.; Kühnel, R.S.; Rentsch, D.; Remhof, A.; Hagemann, H.; Battaglia, C. A highly stable sodium solid-state electrolyte based on a dodeca/deca-borate equimolar mixture. *Chem. Commun.* **2017**, *53*, 4195–4198. [CrossRef]
18.  Cao, K.; Zhang, C.-Y.; Xu, T.-T.; Wu, J.; Wen, X.-Y.; Jiang, W.-J.; Chen, M.; Yang, J. Synthesis of Polyhedral Borane Cluster Fused Heterocycles via Transition Metal Catalyzed B-H Activation. *Molecules* **2020**, *25*, 391. [CrossRef]
19.  Stogniy, M.Y.; Erokhina, S.A.; Sivaev, I.B.; Bregadze, V.I. Nitrilium derivatives of polyhedral boron compounds (boranes, carboranes, metallocarboranes): Synthesis and reactivity. *Phosphorus Sulfur Silicon Relat. Elem.* **2019**, *194*, 983–988. [CrossRef]
20.  Shmal'ko, A.V.; Sivaev, I.B. Chemistry of Carba-closo-decaborate Anions [$CB_9H_{10}]^-$ (Review). *Russ. J. Inorg. Chem.* **2019**, *64*, 1726–1749. [CrossRef]
21.  Bregadze, V.I.; Sivaev, I.B.; Dubey, R.D.; Semioshkin, A.; Shmal'ko, A.V.; Kosenko, I.D.; Lebedeva, K.V.; Mandal, S.; Sreejyothi, P.; Sarkar, A.; et al. Boron-Containing Lipids and Liposomes: New Conjugates of Cholesterol with Polyhedral Boron Hydrides. *Chem. Eur. J.* **2020**, *26*, 13832–13841. [CrossRef]
22.  Semioshkin, A.A.; Sivaev, I.B.; Bregadze, V.I. Cyclic oxonium derivatives of polyhedral boron hydrides and their synthetic applications. *J. Chem. Soc. Dalt. Trans.* **2008**. [CrossRef]
23.  Avdeeva, V.V.; Malinina, E.A.; Zhizhin, K.Y.; Kuznetsov, N.T. Structural Diversity of Cationic Copper(II) Complexes with Neutral Nitrogen-Containing Organic Ligands in Compounds with Boron Cluster Anions and Their Derivatives (Review). *Russ. J. Inorg. Chem.* **2020**, *65*, 514–534. [CrossRef]

24. Leyden, R.N.; Hawthorne, M.F. Synthesis of diazonium derivatives of decahydrodecaborate(2-) from arylazo intermediates. *Inorg. Chem.* **1975**, *14*, 2444–2446. [CrossRef]

25. Hertler, W.R.; Knoth, W.H.; Muetterties, E.L. Chemistry of Boranes. XXIV. Carbonylation of Derivatives of $B_{10}H_{10}{}^{2-}$ and $B_{12}H_{12}{}^{2-}$ with Oxalyl Chloride. *Inorg. Chem.* **1965**, *4*, 288–293. [CrossRef]

26. Jelinek, T.; Štibr, B.; Mareš, F.; Plešek, J.; Heřmánek, S. Halogenation of 4,5-dicarba-arachno-nonaborane(13),4,5-$C_2B_7H_{13}$. *Polyhedron* **1987**, *6*, 1737–1740. [CrossRef]

27. Frank, R.; Adhikari, A.K.; Auer, H.; Hey-Hawkins, E. Electrophile-Induced Nucleophilic Substitution of the nido-Dicarbaundecaborate Anion nido-7,8-$C_2B_9H_{12}$—By Conjugated Heterodienes. *Chem. Eur. J.* **2014**, *20*, 1440–1446. [CrossRef] [PubMed]

28. Vatsadze, S.Z.; Medved'ko, A.V.; Bodunov, A.A.; Lyssenko, K.A. Bispidine-based bis-azoles as a new family of supramolecular receptors: The theoretical approach. *Mendeleev Commun.* **2020**, *30*, 344–346. [CrossRef]

29. Giba, I.S.; Tolstoy, P.M. Self-assembly of hydrogen-bonded cage tetramers of phosphonic acid. *Symmetry* **2021**, *13*, 258. [CrossRef]

30. Jiang, P.; Record, M.C.; Boulet, P. Electron density and its relation with electronic and optical properties in 2D Mo/W dichalcogenides. *Nanomaterials* **2020**, *10*, 2221. [CrossRef] [PubMed]

31. Sethio, D.; Daku, L.M.L.; Hagemann, H.; Kraka, E. Quantitative Assessment of B–B–B, B–$H_b$–B, and B–$H_t$ Bonds: From $BH_3$ to $B_{12}H_{12}{}^{2-}$. *ChemPhysChem* **2019**, *20*, 1967–1977. [CrossRef] [PubMed]

32. Bader, R.; Legare, D. Properties of atoms in molecules: Structures and reactivities of boranes and carboranes. *Can. J. Chem.* **1992**, *70*, 657–677. [CrossRef]

33. Voinova, V.V.; Selivanov, N.A.; Plyushchenko, I.V.; Vokuev, M.F.; Bykov, A.Y.; Klyukin, I.N.; Novikov, A.S.; Zhdanov, A.P.; Grigoriev, M.S.; Rodin, I.A.; et al. Fused 1,2-Diboraoxazoles Based on closo-Decaborate Anion-Novel Members of Diboroheterocycle Class. *Molecules* **2021**, *26*, 248. [CrossRef] [PubMed]

34. Klyukin, I.N.; Novikov, A.S.; Zhdanov, A.P.; Zhizhin, K.Y.; Kuznetsov, N.T. Theoretical study of closo-borate derivatives of general type $[B_nH_{n-1}COR]^{2-}$ (n = 6, 10, 12; R = H, $CH_3$, $NH_2$, OH, $OCH_3$)—Borylated analogue of organic carbonyl compounds. *Polyhedron* **2020**, *187*, 114682. [CrossRef]

35. Klyukin, I.N.; Novikov, A.S.; Zhdanov, A.P.; Zhizhin, K.Y.; Kuznetsov, N.T. Theoretical study of monocarbonyl derivatives of closo-borate anions $[B_nH_{n-1}CO]^-$ (n = 6, 10, 12): Bonding and reactivity analysis. *Mendeleev Commun.* **2020**, *30*, 88–90. [CrossRef]

36. Geerlings, P.; Chamorro, E.; Chattaraj, P.K.; De Proft, F.; Gázquez, J.L.; Liu, S.; Morell, C.; Toro-Labbé, A.; Vela, A.; Ayers, P. Conceptual density functional theory: Status, prospects, issues. *Theor. Chem. Acc.* **2020**, *139*, 36. [CrossRef]

37. Geerlings, P.; De Proft, F.; Langenaeker, W. Conceptual density functional theory. *Chem. Rev.* **2003**, *103*, 1793–1873. [CrossRef]

38. Domingo, L.R.; Ríos Gutiérrez, M.; Castellanos Soriano, J. Understanding the Origin of the Regioselectivity in Non-Polar [3+2] Cycloaddition Reactions through the Molecular Electron Density Theory. *Organics* **2020**, *1*, 19–35. [CrossRef]

39. Allgäuer, D.S.; Jangra, H.; Asahara, H.; Li, Z.; Chen, Q.; Zipse, H.; Ofial, A.R.; Mayr, H. Quantification and Theoretical Analysis of the Electrophilicities of Michael Acceptors. *J. Am. Chem. Soc.* **2017**, *139*, 13318–13329. [CrossRef]

40. Wang, Y.; Zhang, C.; Zhao, Y.L.; Zhao, R.; Houk, K.N. Understand the specific regio-and enantioselectivity of fluostatin conjugation in the post-biosynthesis. *Biomolecules* **2020**, *10*, 815. [CrossRef]

41. Fuentealba, P.; Florez, E.; Tiznado, W. Topological Analysis of the Fukui Function. *J. Chem. Theory Comput.* **2010**, *6*, 1470–1478. [CrossRef]

42. Rodríguez-Zavala, J.G. Local reactivity through fukui function on endohedral mono-metallofullerenes. *Phys. E Low-Dimens. Syst. Nanostruct.* **2019**, *105*, 186–195. [CrossRef]

43. Kochnev, V.K.; Avdeeva, V.V.; Malinina, E.A.; Kuznetsov, N.T. Theoretical study of H2 Elimination from $[B_nH_{n+1}]$ monoanions (n = 6–9, 11). *Russ. J. Inorg. Chem.* **2014**, *59*, 1268–1275. [CrossRef]

44. Sivaev, I.B.; Semioshkin, A.A.; Brellochs, B.; Sjoberg, S.; Bregadze, V.I. Synthesis of oxonium derivatives of the dodecahydro–closo-dodecaborate anion $[B_{12}H_{12}]^{2-}$. Tetramethylene oxonium derivative of $[B_{12}H_{12}]^{2-}$ as a convenient precursor for the synthesis of functional compounds for boron neutron capture therapy. *Polyhedron* **2000**, *19*, 627–632. [CrossRef]

45. Sivaev, I.B.; Prikaznov, A.V.; Naoufal, D. Fifty years of the closo-decaborate anion chemistry. *Collect. Czechoslov. Chem. Commun.* **2010**, *75*, 1149–1199. [CrossRef]

46. Hehre, W.J.; Ditchfield, K.; Pople, J.A. Self-consistent molecular orbital methods. XII. Further extensions of gaussian-type basis sets for use in molecular orbital studies of organic molecules. *J. Chem. Phys.* **1972**, *56*, 2257–2261. [CrossRef]

47. Da Chai, J.; Head-Gordon, M. Long-range corrected hybrid density functionals with damped atom-atom dispersion corrections. *Phys. Chem. Chem. Phys.* **2008**, *10*, 6615–6620. [CrossRef] [PubMed]

48. Nikolova, V.; Cheshmedzhieva, D.; Ilieva, S.; Galabov, B. Atomic Charges in Describing Properties of Aromatic Molecules. *J. Org. Chem.* **2019**, *84*, 1908–1915. [CrossRef]

49. Oller, J.; Pérez, P.; Ayers, P.W.; Vöhringer-Martinez, E. Global and local reactivity descriptors based on quadratic and linear energy models for α, β -unsaturated organic compounds. *Int. J. Quantum Chem.* **2018**, *118*, e25706. [CrossRef]

50. Makhyoun, M.A.; Massoud, R.A. Theoretical calculation of the exchange coupling constant in some polymeric nickel(II) complexes using range-separated functionals. *Eur. J. Chem.* **2018**, *9*, 382–385. [CrossRef]

51. Neese, F. The ORCA program system. *WIREs Comput. Mol. Sci.* **2012**, *2*, 73–78. [CrossRef]

52. Glendening, J.K.E.D.; Badenhoop, A.E.R.; Carpenter, J.E.; Bohmann, J.A.; Morales, P.K.C.M.; Landis, C.R.; Weinhold, T.C.I.F. *NBO 7.0*; University of Wisconsin: Madison, WI, USA, 2018.

53. Bader, R.F.W. *Atoms in Molecules: A Quantum Theory*; Oxford University Press: Oxford, UK, 1990.
54. Lu, T.; Chen, F. Multiwfn: A Multifunctional Wavefunction Analyzer. *J. Comp. Chem.* **2011**, *33*, 580–592. [CrossRef]
55. Parr, R.G.; Szentpály, L.V.; Liu, S. Electrophilicity Index. *J. Am. Chem. Soc.* **1999**, *121*, 1922–1924. [CrossRef]
56. Kononova, E.G.; Leites, L.A.; Bukalov, S.S.; Pisareva, I.V.; Chizhevsky, I.T. Experimental and theoretical study of the vibrational spectrum, structure and electron density distribution of neutral 11-vertex dicarbaborane 2,3-$C_2B_9H_{11}$. *J. Mol. Struct.* **2006**, *794*, 148–153. [CrossRef]
57. Vologzhanina, A.V.; Korlyukov, A.A.; Avdeeva, V.V.; Polyakova, I.N.; Malinina, E.A.; Kuznetsov, N.T. Theoretical QTAIM, ELI-D, and Hirshfeld Surface Analysis of the $Cu-(H)B$ Interaction in [$Cu_2(bipy)_2B_{10}H_{10}$]. *J. Phys. Chem. A* **2013**, *2*, 13138. [CrossRef] [PubMed]
58. Domingo, L.R.; Ríos-Gutiérrez, M.; Pérez, P. Applications of the conceptual density functional theory indices to organic chemistry reactivity. *Molecules* **2016**, *21*, 748. [CrossRef]
59. Domingo, L.R.; Aurell, M.J.; Pérez, P.; Contreras, R. Quantitative characterization of the global electrophilicity power of common diene/dienophile pairs in Diels-Alder reactions. *Tetrahedron* **2002**, *58*, 4417–4423. [CrossRef]